Microelectronics Reliability xxx (2015) xxx–xxx

Contents lists available at ScienceDirect

Microelectronics Reliability

journal homepage: www.elsevier.com/locate/mr

Failure mechanisms of microbolometer thermal imager sensors using chip-scale packaging

Michael Elßner [a,*], Holger Vogt [b]

[a] Fraunhofer IMS, Finkenstraße 61, 47057 Duisburg, Germany
[b] University of Duisburg-Essen, Forsthausweg 2, 47057 Duisburg, Germany

ARTICLE INFO

Article history:
Received 19 May 2015
Received in revised form 20 July 2015
Accepted 20 July 2015
Available online xxxx

Keywords:
Vacuum quality
Hermetic packaging
Micro bolometer
Infrared imager
Reliability
Failure mechanisms
Degradation

ABSTRACT

This paper analyzes relevant failure mechanisms for microbolometer thermal imager sensors that are assembled with a small size and low cost chip scale package. The analyses focus on device specific elements like the bolometer sensor structures, the longtime stability of the sensor and its performance, and the stability of the hermetic chip scale package. Executed reliability tests showed a high reliability of the sensor and the package without hard failures. The package survived harsh environmental accelerated stress tests and showed only a slight reduction of the shear strength through void formation and small cracks within the lead frame that could be verified through FEM simulations. The stress on the bolometers is investigated by thermomechanical FEM simulations. Executed reliability tests showed no enlargement in the number of defect pixel. The sensor performance showed a long-time drift and temperature dependence through outgassing processes inside the package leading to a significant performance reduction. Thus this effect is investigated more closely and possible countermeasures are proposed.
© 2015 Elsevier Ltd. All rights reserved.

1. Infrared thermal imager sensors

Uncooled infrared imagers (IRFPA, infrared focal plane array) (Fig. 1) measure the infrared radiation emitted by warm objects in a typical wavelength range between 8 μm and 14 μm to image temperature distributions of a scene. These IR imagers operate passively without additional active illumination of a scene.

Commercial IRFPAs are based on microbolometers as sensor elements (pixels). They absorb electromagnetic infrared radiation and thus increase their membrane temperature. This leads to a change in the electrical resistance which is converted by a read-out circuit (ROIC) into an electric voltage or a digital value. By using several bolometers forming a pixel array, the thermal radiation of a scene can be measured and imaged.

Uncooled IR (infrared) imagers basically consist of a microbolometer array as an IR image sensor and a hermetic vacuum package with IR-entry window. The needed thermal isolation of the bolometer membrane is realized by constructing a 3D beam or leg structure (Figs. 2, 3) and through the package internal vacuum pressure lower then 10^{-2} mbar. Amorphous silicon (a-Si) and vanadium oxide (VOx) are commonly used as sensor materials. Both are amorphous materials with a high temperature coefficient (TCR).

Actual literature of infrared sensors provides no concrete information about reliability issues. Books on infrared sensors from Budzier [2], Kruse [3] and Rogalski [4] give detailed physical and technical information on infrared sensors but nothing on reliability and long-term stability. Manufacturers like DRS Technologies Inc. [5], BAE Systems [6] and [7] Raytheon Vision Systems [8], describe recent developments and technologies in their publications but provide no concrete information on reliability. Thus the issues of reliability and failure mechanism are described in this paper.

2. Failure mechanisms

In the following the relevant failure mechanisms of infrared imagers will be examined. Typical failures are: electrical failure, leaking package, defective bolometer pixels, performance reduction or assembly problems.

Electrical defects of the ROIC or classic assembly errors like die attachment and bond wire failures are manufacturer specific, state of the art, and not considered here in detail. This paper focuses on the package, the bolometer and the performance degradation.

Studying the literature for reliability concerns it can be stated that infrared sensors have very severe requirements on the internal pressure and require a long-term stability at a pressure of about 10^{-3} mbar acc. to Moraja [9] or Roxhed [10]. Studies of infrared sensors by Niklaus et al. in [11,12] identify a reliable hermetic package as the most important reliability issue. The package internal pressure of less than

* Corresponding author.
E-mail address: michael.elssner@ims.fraunhofer.de (M. Elßner).

http://dx.doi.org/10.1016/j.microrel.2015.07.040
0026-2714/© 2015 Elsevier Ltd. All rights reserved.

Please cite this article as: M. Elßner, H. Vogt, Failure mechanisms of microbolometer thermal imager sensors using chip-scale packaging, Microelectronics Reliability (2015), http://dx.doi.org/10.1016/j.microrel.2015.07.040

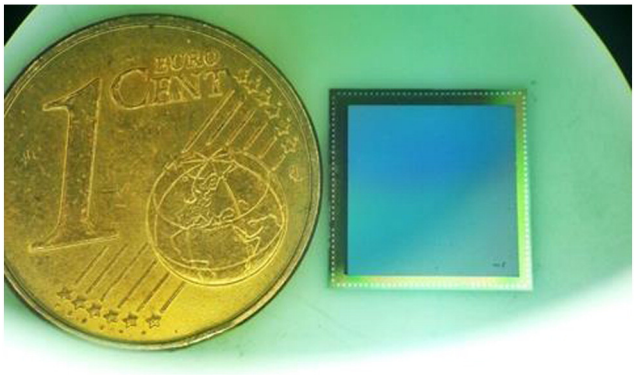

Fig. 1. Fraunhofer IMS infrared imager in QVGA size.

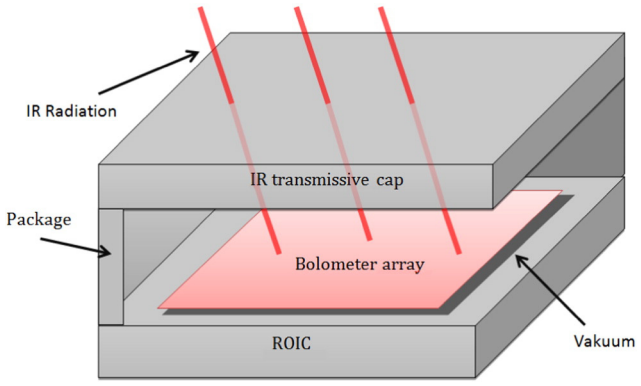

Fig. 2. SEM picture of a bolometer array in a top view (left) and a side view (right) [1].

0.01 mbar [11] has to be constant over the devices' lifetime. In addition, the transmission of the infrared window must remain constant. The hermeticity and low outgassing rates are most important acc. to Premachandran [13].

3. Performance degradation

Performance degradation is a serious matter. Even at 20 °C room temperature a significant performance loss over one year storage could be measured. The performance is described after [14–16] by the responsivity R (sensor sensitivity) and the noise-equivalent temperature difference $NETD$ by the following equations:

$$NETD = \frac{4 \cdot F_Z^2 \cdot U_n}{R \cdot A_B \cdot \phi \cdot \left(\frac{\Delta P}{\Delta T}\right)} \tag{0.1}$$

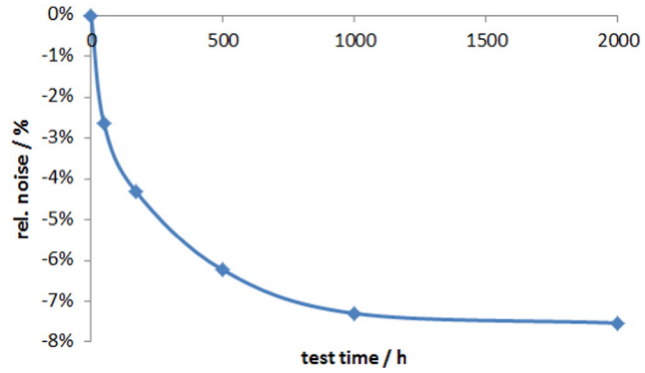

Fig. 4. Measured relative noise voltage changes ΔU_n by HTOL testing with 115 °C and electrical stimulation.

$$R = \frac{\mathrm{TCR} \cdot \beta \cdot \varepsilon \cdot U_{\mathrm{Bolo}}}{G_{\mathrm{Th}} \cdot \sqrt{1 + \omega^2 \cdot \tau^2}}. \tag{0.2}$$

Here F_Z is the F-number of the infrared optics, U_n the noise voltage, A_B the bolometer pixel area, ϕ the transmission coefficient, $\Delta P/\Delta T$ the temperature contrast, TCR the temperature coefficient of resistance, β the bolometer fill factor, ε the absorption coefficient, U_{Bolo} the bolometer voltage, G_{Th} the thermal conductivity, ω the reciprocal of the frame frequency and τ the thermal time constant.

Parameters that could shift over the lifetime and thus lower the sensor performance are the noise voltage U_n, the TCR, the optical transmission ϕ and the thermal conductivity G_{Th}. These parameters are consequently analyzed separately.

3.1. Noise

Executed HTOL (high temperature operating life) test by 115 °C over 2000 h showed a reduction of the noise level, which has a positive effect on the *NETD*. The calculated average of the relative noise changes of 30 devices are shown in Fig. 4. Here the noise is defined as the average standard deviation of the digital values measured over 50 frames.

3.2. Transmission

In the second step the infrared caps of the chip scale package were analyzed separately. Despite intense aging with 350 h autoclave (121 °C, 100% RH), 500 h storage at 200 °C or 1000 temperature cycles from −50 to +150 °C, no reduction of the infrared transmission could be measured by Fourier transform infrared spectroscopy (FTIR).

3.3. TCR

The TCR was evaluated on sensor devices in measuring the electrical resistance over different temperatures with an accuracy of ca. 0.5%.

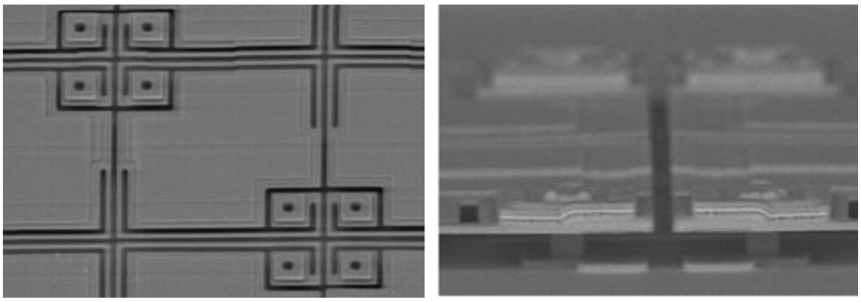

Fig. 3. Principle of construction of an infrared imager.

Please cite this article as: M. Elßner, H. Vogt, Failure mechanisms of microbolometer thermal imager sensors using chip-scale packaging, Microelectronics Reliability (2015), http://dx.doi.org/10.1016/j.microrel.2015.07.040

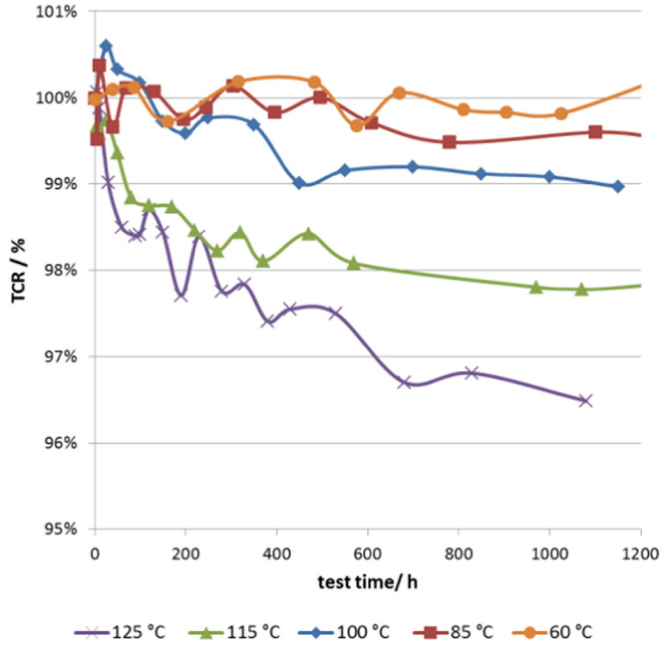

Fig. 5. Measured relative TCR changes after thermal aging at different temperatures.

The measurements in Fig. 5 show the temperature dependent degradation of the TCR. But in relation to the overall performance degradation (Fig. 6), the reduction of the TCR is quite low and has a ratio of about 10%. For example the responsivity after 1000 h at 125 °C is decreased by 22.5% and the TCR by 2.8% (Fig. 6). The complete performance degradation cannot be explained by the TCR and thus must mainly be caused by the thermal insulation.

3.4. Thermal conductivity

As described in [17] the thermal conductivity of the package depends on the number of gas molecules and thus on the package internal pressure.

a) Gas analyses

The package internal gas composition was analyzed by time-of-flight mass spectroscopy. But the absolute pressure could not be measured.

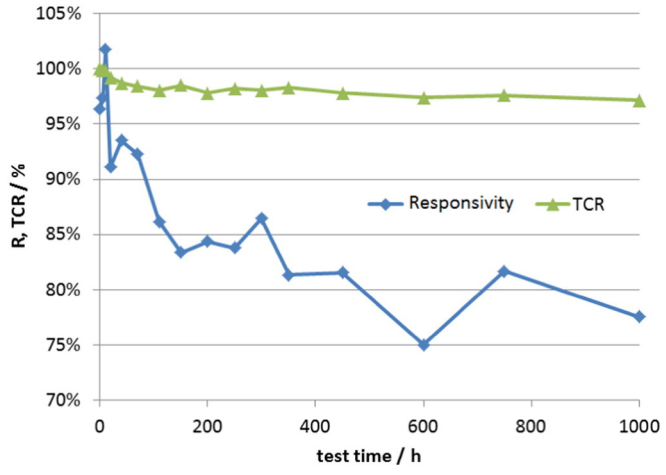

Fig. 6. Relative changes in the responsivity and TCR at HTOL 125 °C for 1000 h.

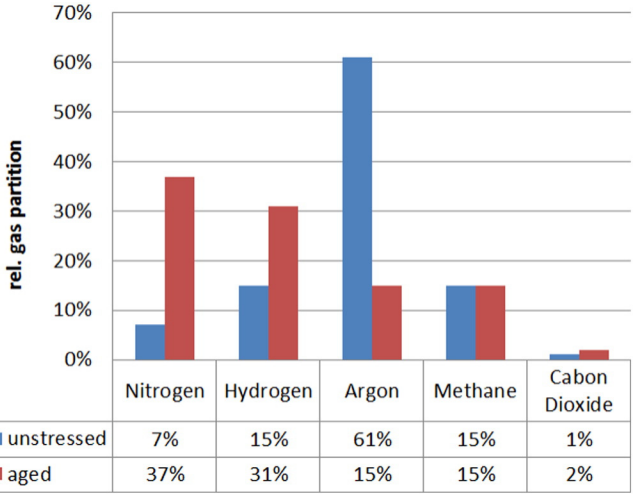

	Nitrogen	Hydrogen	Argon	Methane	Cabon Dioxide
unstressed	7%	15%	61%	15%	1%
aged	37%	31%	15%	15%	2%

Fig. 7. Comparison of the relative gas composition before and after thermal aging by 2000 h 150 °C.

A graphical comparison of the gas composition is depicted in Fig. 7. It should be noted that in this figure the relative gas composition is indicated. This means for example that the argon fraction after aging is not really reduced, but the other parts and the total gas amount are grown. The initial portion of argon with about 60% is very high, but it decreases after aging to 15%. As argon is a rare gas and cannot diffuse through metals and is not absorbed by getter materials, the absolute amount of argon gas should remain constant. Consequently, the remaining gasses must have increased. The most outgassing are nitrogen and hydrogen, followed by hydrocarbons and carbon dioxide.

b) Package internal pressure

A method and highly accurate measuring system for the package internal pressure of a bolometer imager is described by Elßner in [17]. Further described are the physical backgrounds, the outgassing processes, the thermal conductivities, pressure calculation and measurement results.

This vacuum evaluation method is used to monitor the thermal isolation and the package internal pressure. A comparison of normalized curves of the responsivity (R) and the measured values from

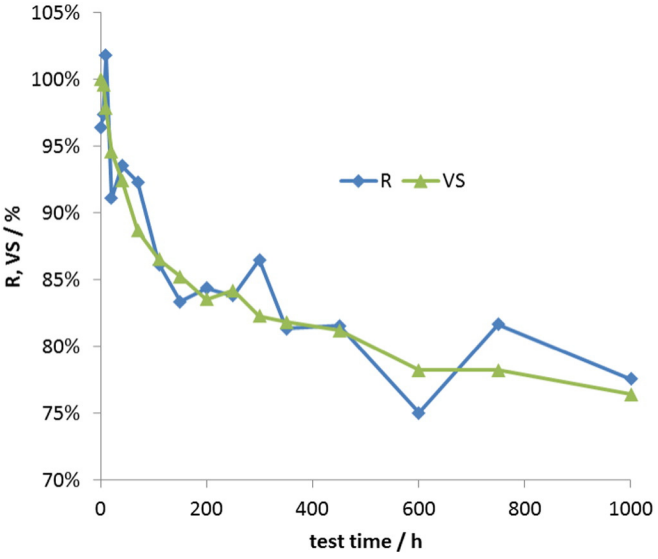

Fig. 8. Degradation curves of the responsivity *R* and package pressure measured by the vacuum sensor *VS* before and after thermal aging by 125 °C.

Please cite this article as: M. Elßner, H. Vogt, Failure mechanisms of microbolometer thermal imager sensors using chip-scale packaging, Microelectronics Reliability (2015), http://dx.doi.org/10.1016/j.microrel.2015.07.040

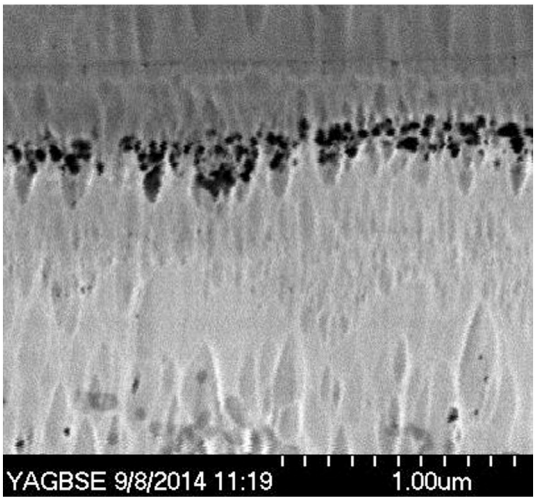

Fig. 9. Void formation in thermally aged eutectic lead frame cross section.

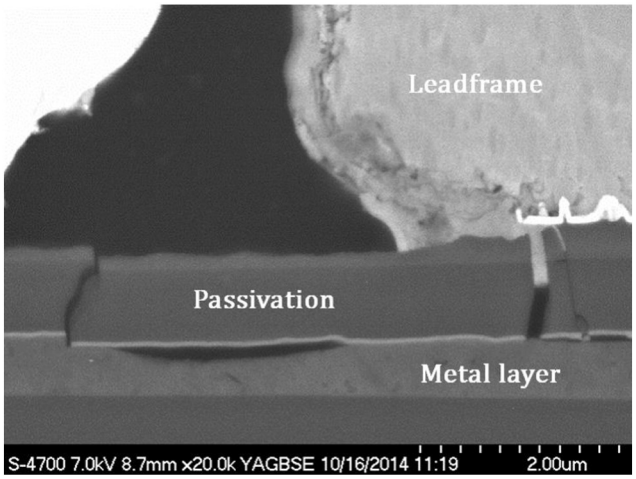

Fig. 11. Cracks after aging in the passivation beside the leadframe.

the vacuum sensor (VS) by a thermal aging of 125 °C shows (Fig. 8) that both have the same degradation curve. This proves that a reduction in the thermal insulation and thus pressure reduces the performance. With this method, the degradation of the TCR is also detected so that the overall degradation is measured. Consequently the infrared sensors' performance degradation is related to an increasing package pressure and a slight reduction of the TCR.

Countermeasures have to be taken to reduce the impact of outgassing and thus sensor degradation such as bake-out before package sealing, increasing the package volume for example through etching a cavity in cap wafer and the optimized use of getter layers with activation temperatures adapted to the packaging process on the biggest area possible. If possible the getter material is electrically contactable and thus capable of being activated after sealing by joule heating.

4. Reliability of the chip scale package

The analyzed hermetically sealed vacuum chip scale packages manufactured and developed by Fraunhofer IMS have a size of 9 × 9 mm and use a eutectic leadframe to solder an infrared transmissive cap chip on the substrate wafer. The packages were stressed with sinusoidal vibrations of 20 G, mechanical shocks of 500 G in 1 ms, 264 h in the autoclave by 121 °C and 100% RH, and 1000 thermal cycles by −65 °C to +175 °C. None of these stress tests led to failure or a loss of the hermeticity of the package proving the high reliability of the chip scale package.

a) Shear tests

The infrared sensors were also tested by shear tests, where the cap chip is sheared and the force measured over 5 samples for each test. Temperature storage at 150 °C over 1700 h led to a reduction of the shear force by 12% and 1250 thermal cycles from −50 °C/+150 °C to 18%.

b) Material analysis of leadframe

Packages aged by 1000 thermal cycles from −50 °C/+150 °C were mechanically sawed and polished and additionally polished by ion beams, to analyze the cross section of the leadframe by electron microscopy.

The analyzed cross section (Fig. 9) showed void formation at the interface between the eutectic and nickel film. Further analyses by energy-dispersive X-ray spectroscopy (EDX) showed that nickel diffused into the eutectic because of the different diffusion coefficients leading to void formation. Furthermore smaller cracks between the leadframe and the silicon (Fig. 10) and passivation cracks beside the leadframe (Fig. 11) could be observed. This stress could also be verified through thermo-mechanical simulation (Fig. 12) with finite element methods (FEM) using COMSOL multiphysics.

The micro damages appearing after this intense aging would explain the reduced shear strength. However, these damages are moderate in relation to the structure sizes and thus far away from a structural failure.

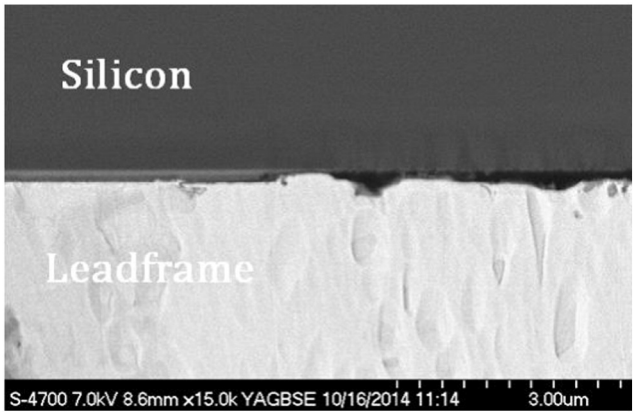

Fig. 10. Crack formation between the leadframe and silicon interface.

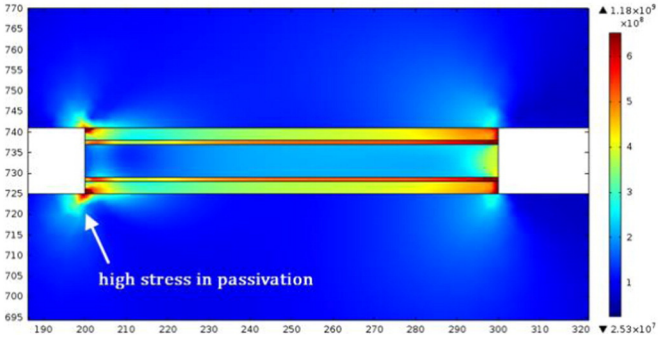

Fig. 12. 2D FEM simulation of Von-Mises-stress by 150 °C.

Please cite this article as: M. Elßner, H. Vogt, Failure mechanisms of microbolometer thermal imager sensors using chip-scale packaging, Microelectronics Reliability (2015), http://dx.doi.org/10.1016/j.microrel.2015.07.040

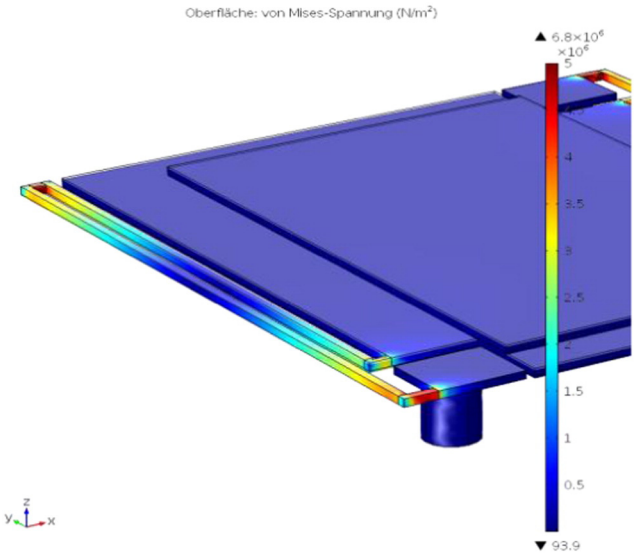

Fig. 13. FEM bolometer simulation model by acceleration of 1000 G, maximum von-Mises-stress is 6.8 MPa.

5. Bolometer

Finally the bolometer sensor elements are investigated. Executed reliability tests like vibrations, mechanical shocks, thermal cycles and thermal aging as mentioned earlier showed no damages. Additional executed FEM simulations as in Fig. 13 showed no remarkable stress within the bolometer structures. The simulated Von-Mises-stress is far below the critical maximum tensile strength of silicon oxide (8.4 GPa [18]).

6. Conclusion

The chip scale package showed only minor cracks and a void formation that slightly reduces the mechanical strength. The bolometer sensor elements showed no failures by accelerated aging and FEM simulations. Despite the intense accelerated aging, package and bolometers showed no failures and are consequently highly reliable. The dominant failure mechanism is the loss of the bolometer's thermal insulation. The temperature dependent performance degradation through outgassing processes inside the package is leading to an increased package pressure and thus to a decreasing responsivity over time. Furthermore a decreasing noise level could be measured that partially compensates for the responsivity losses for the *NETD* value.

Acknowledgments

This research was supported by the Fraunhofer Institute for Microelectronic Circuits and Systems (IMS) and the University of Duisburg-Essen.

References

[1] Fraunhofer IMS, Annual report of the Fraunhofer-Institute for microelectronic circuits and systems IMS Duisburg 2013(Online, available) http://www.ims.fraunhofer.de/fileadmin/user/presse/jahresberichte/IMS_AnnualReport2011_klein.pdf2013.
[2] H. Budzier, G. Gerlach, Thermal Infrared Sensors: Theory, Optimisation and Practice, John Wiley & Sons, 2011.
[3] P. Kruse, D. Skatrud, Uncooled infrared imaging arrays and systems, Semiconductors and Semimetals, vol. 47, Academic Press, 1997.
[4] A. Rogalski, Infrared Detectors, 2nd ed. CRC Press, 2010.
[5] C. Li, G. Skidmore, et al., Recent development of ultra small pixel uncooled focal plane arrays at DRS, Proc. SPIE 6542, Infrared Technology and Applications XXXIII2007. 65421Y.
[6] B. Backer, M. Kohin, Advances in uncooled technology at BAE Systems, Proc. SPIE 5074, Infrared Technology and Applications XXIX 2003, p. 548.
[7] R. Blackwell, T. Bach, et al., 17 μm pixel 640 × 480 microbolometer FPA development at BAE Systems, Proc. SPIE 6542, Infrared Technology and Applications XXXIII 2007, p. 65421U.
[8] D. Murphy, M. Ray, J. Wyles, et al., 640 × 512 17 μm microbolometer FPA and sensor development, Proc. SPIE 6542, Infrared Technology and Applications XXXIII 2007, p. 65421Z.
[9] M. Moraja, M. Amiotti, H. Florence, Chemical treatment of getter films on wafers prior to vacuum, reliability, testing, and characterization of MEMS/MOEMS III, Proc. SPIE 5343 (2004).
[10] N. Roxhed, F. Niklaus, A. Fischer, et al., Low-cost uncooled microbolometers for thermal imaging, Optical Sensing and Detection, Proc. of SPIE, vol. 77262010. 772611-1.
[11] F. Niklaus, C. Jansson, A. Decharat, S. G., Performance model for uncooled infrared bolometer arrays and performance predictions of bolometers operating at atmospheric pressure, Infrared Phys. Technol. (2007)http://dx.doi.org/10.1016/j.infrared.2007.08.001.
[12] F. Niklaus, C. Vieider, H. Jakobsen, MEMS-based uncooled infrared bolometer arrays — a review, Proc. of SPIE, vol. 6836 2007, p. 68360D-1.
[13] C. Premachandran, C. Chong, T. Chai, M. Iyer, Vacuum packaging development and testing for an uncooled IR bolometer device, Proc. 54th Electron. Compon. Technol. Conf 2004, pp. 951–955.
[14] P.W. Kruse, Uncooled IR focal plane arrays, Opto-Electron. Rev. 7 (1999).
[15] P.L. Marasco, E.L. Dereniak, Uncooled infrared sensor performance, Proc. SPIE 2020 (1993) (San Diego, USA).
[16] R.A. Wood, Uncooled microbolometer infrared sensor arrays, Infrared Emitters and Detectors. , Kluwer Academic Publishers, Norwell, Massachusetts, 2001.
[17] M. Elßner, Vacuum quality evaluation for uncooled micro bolometer thermal imager sensors, European Symposium on the Reliability of Electron Devices, Failure Physics and Analysis (ESREF) <25, Berlin, 2014.
[18] M. Madou, Fundamentals of Microfabrication, CRC Press, 1997.

Please cite this article as: M. Elßner, H. Vogt, Failure mechanisms of microbolometer thermal imager sensors using chip-scale packaging, Microelectronics Reliability (2015), http://dx.doi.org/10.1016/j.microrel.2015.07.040